ULTRASOUND NEWS

October 2023

Ahead of print

Med Ultrason 2023:0, 1-3 Online first
DOI: 10.11152/mu-4127

Ultrasound description and follow up of painful cervical interspinous bursitis in a Polymyalgia Rheumatica patient – a case report

Plamen Todorov, Anastas Zgurov Batalov

Rheumatology Clinic, "Kaspela" University Hospital, Medical University of Plovdiv, Plovdiv, Bulgaria

Abstract

We present a Polymyalgia Rheumatica (PMR) case with active Cervical Interspinous Bursitis (CIB) causing debilitating neck pain as the most intensive symptom of the disease as reported by the patient. CIB was diagnosed and followed by Musculoskeletal Ultrasound (MSUS). MSUS examination of patient's posterior cervical region reviled well demarcated an-/hypoechoic lesions around and cranially of the spinous processes of the sixth and seventh cervical vertebra. The initial detailed sonographic characteristics of the CIB are described, as well as the evolution of lesions size and extent with the treatment and patient's clinical improvement. To our knowledge this is the first detailed sonographic description of CIB in PMR.

Keywords: Cervical Bursitis; Ultrasound; Polymyalgia Rheumatica

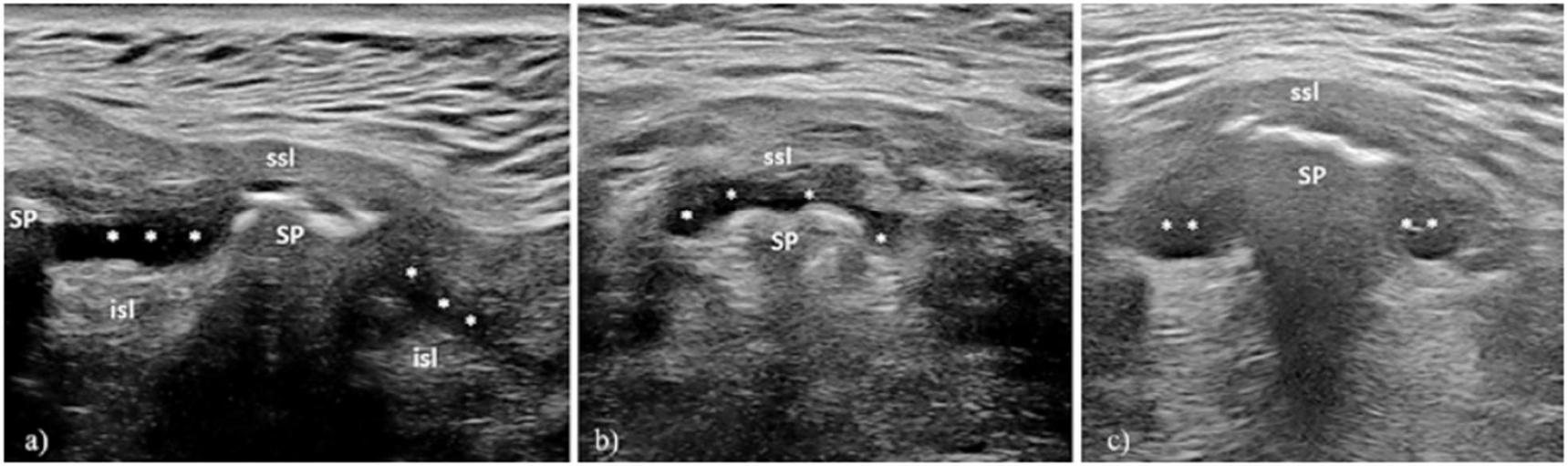

Fig 1. a) Longitudinal midline scan of the cervical spine at C6 and C7 level; b) transverse scan at C6 level; c) transverse scan at the C7 level. There is an-/ hypoechoic well-delineated lesions (asterisks) over and between the spinous processes. The lesions expand in the paramedian space, more at C7 level. SP, spinous processes; SSL, supraspinous ligament; ISL, interspinous ligament; L, lamina.

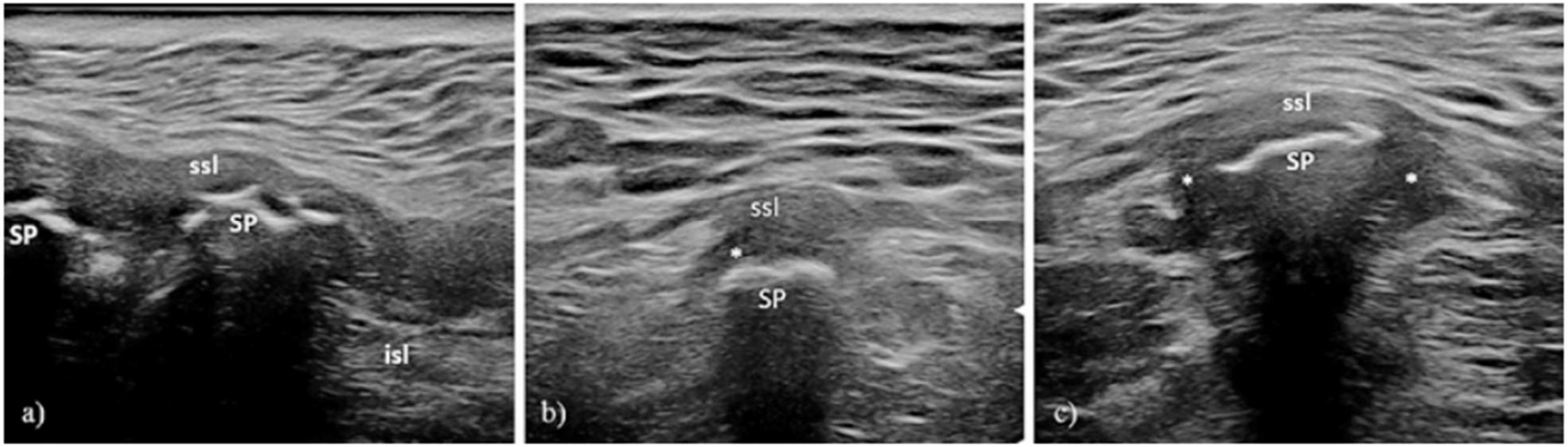

Fig 2. a) Longitudinal; b) and c) transverse scans at the same levels as in figure 1, one month later. The size and expansion of the lesions have decreased significantly (asterisks). (Abbreviations – see Fig 1)

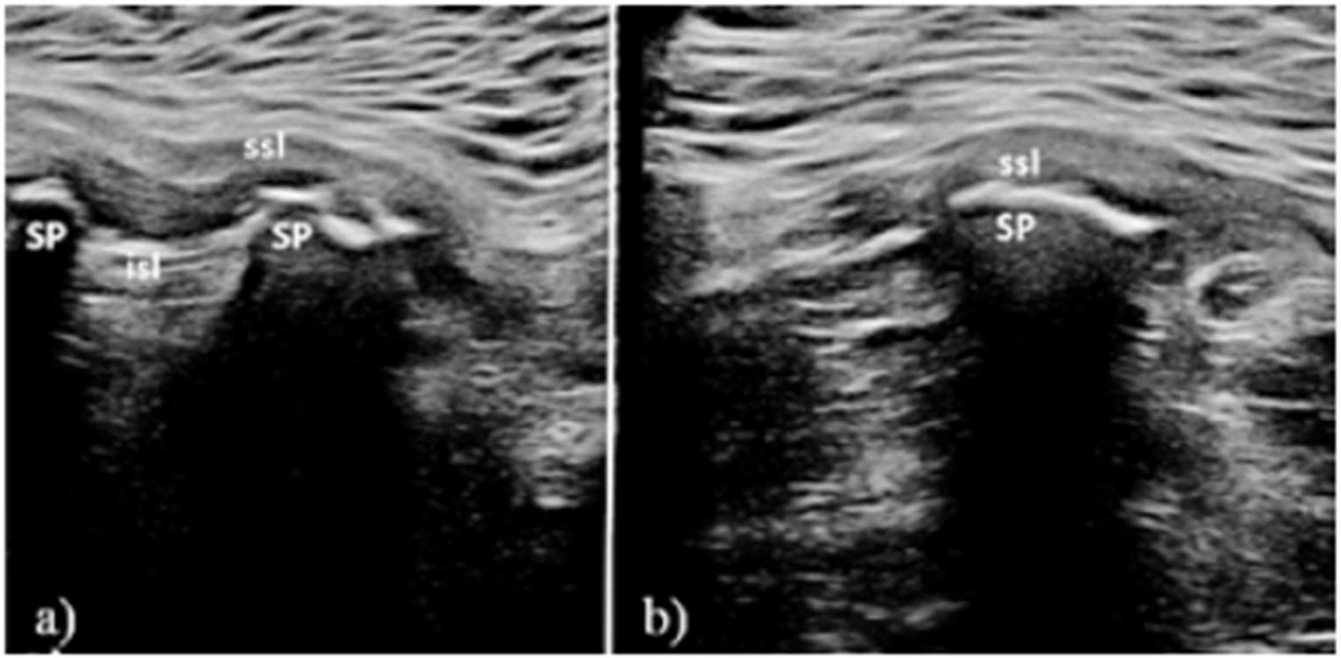

Fig 3. a) Longitudinal and b) transverse scan at the same levels appr. two months later confirmed complete resolution of the described lesions. (Abbreviations – see Fig 1)

Review

Med Ultrason 2023, Vol. 25, no. 3, 325-329
DOI: 10.11152/mu-4060

Sono-palpation and sono-Tinel in musculoskeletal ultrasound examination: use all "sono-senses". A systematic review

Carmelo Pirri[1], Nina Pirri[2], Carla Stecco[1], Veronica Macchi[1], Andrea Porzionato[1], Raffaele De Caro[1], Levent Özçakar[3]

[1]Department of Neurosciences, Institute of Human Anatomy, University of Padova, Padua, Italy, [2]Department of Medicine-DIMED, School of Radiology, Radiology Institute, University of Padua, Padova, Italy, [3]Department of Physical and Rehabilitation Medicine, Hacettepe University Medical School, Ankara, Turkey

Abstract

Flexibility and dynamic perspective of ultrasound imaging allow for a targeted/focused examination, yielding extra findings. Sonopalpation – also referred as sono-Tinel for nerves – is one of those particular features of ultrasound examination whereby the ultrasound probe is actively 'manipulated'. It is paramount to ascertain the painful structure/pathology during the evaluation of a patient and it is not possible with other imaging techniques other than ultrasonography. In this aspect, the current review aims to provide an analysis of the literature regarding the use of sonopalpation for clinical and research purposes respectively.

Keywords: ultrasonography; probe; muscle; bone; pain

Table I. Exemplary pathologies for the use of sonopalpation

Tissue	**Pathology**
Skin/subcutaneous tissue	Cyst, lipoma
Fascia	Fasciitis
Tendon and ligament	Sprain, (calcific) tendinopathy, enthesopathy
Bursa	Bursitis
Skeletal muscle	Strain, atrophy, myositis ossificans
Joint and capsule	Effusion/synovitis, adhesive capsulitis, loose body (osteochondritis dissecans)
Cartilage	Degeneration, meniscopathy
Peripheral nerve	Entrapment
Bony/periosteum	Erosion and fracture

To the best of our knowledge, this is the first review
about sonopalpation for the evaluation of muscle-skeletal sof tissues.
Our review suggests that sonopalpation is **superior to US or physical examinat**
alone and is very helpful in the diagnosis and management of various
muscle-skeletal soft tissues diseases. This is a commentary that may have
excluded other muscle-skeletal soft issues.
Further studies should be carried out to clearly define the role of sonopalpatio
in diverse clinical conditions.
As a limitation, despite the fact that we systematically conducted a literature
search to reduce selection bias,some studies may have been inevitably omitte
Future prospective high-quality studies on the use of sonopalpation during
neuromusculoskeletal US examination are definitely welcome.

Cocco et al. Insights into Imaging (2022) 13:189
https://doi.org/10.1186/s13244-022-01335-z

Insights into Imaging
EUROPEAN SOCIETY OF RADIOLOGY

EDUCATIONAL REVIEW Open Access

Ultrasound imaging of bone fractures

Giulio Cocco[1], Vincenzo Ricci[2], Michela Villani[3], Andrea Delli Pizzi[3,4*], Jacopo Izzi[3], Marco Mastandrea[3], Andrea Boccatonda[5], Ondřej Naňka[6], Antonio Corvino[7], Massimo Caulo[3,4,5,6,7,8] and Jacopo Vecchiet[9]

Abstract

Ultrasound imaging is widely used to evaluate the neuromusculoskeletal system, and recently, a particular interest is mounting in assessing the bone tissue and fractures. Ultrasound can be considered a valuable diagnostic tool to perform a first-line evaluation of bone tissue, especially in particular settings without direct access to X-ray imaging and/or in emergency conditions. Moreover, different healing phases of bone fractures can be accurately assessed by combining the B-mode modality and (high-sensitive) color/power Doppler optimizing the management of patients—e.g., planning of progressive loads and rehabilitation procedures. In this review, we summarized the role of ultrasound imaging in the management of bone fractures and described the most common sonographic signs encountered in the daily practice by assessing different types of bone fractures and the progressive phases of the healing process.

Key points

- US represents an alternative to XR for the occult bone fractures diagnosis.
- Knowledge of sonographic patterns is crucial for the detection of challenging fractures.
- US allows an early assessment of the callus formation and bone healing.

Keywords: Ultrasound, Bone fracture, Fracture healing

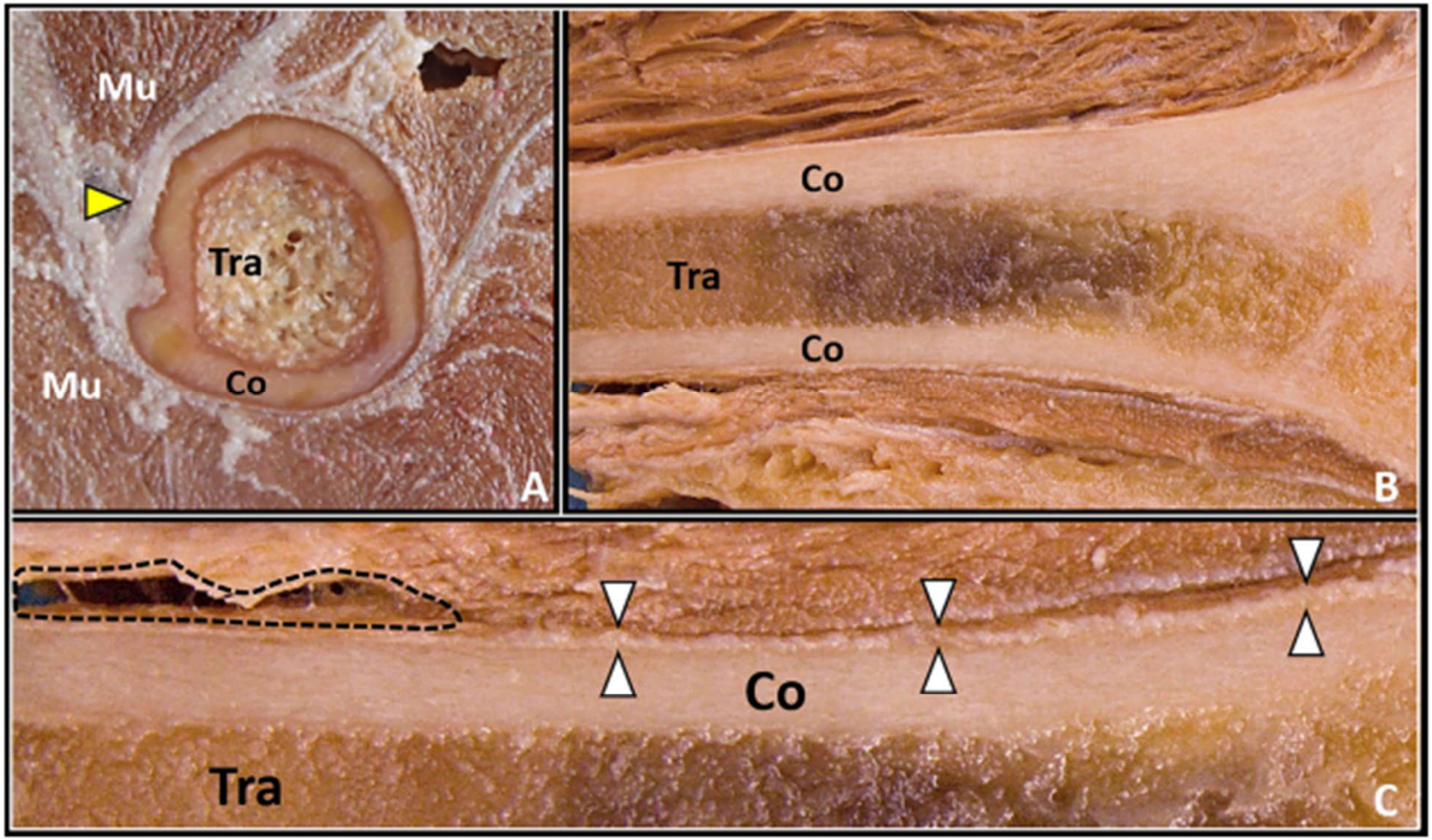

Fig. 1 Cadaveric anatomy of bone tissue. The bone presents an inner portion with a trabecular texture (*Tra*) and an outer component—compact in nature—known as cortical bone (*Co*) (**A**, **B**). Of note, the periosteum (*white arrowheads*) tightly envelops the surface of the bone and, if damaged, allows the blood to diffuse toward the epi-periosteal space (*black dotted line*) (**C**). Mu: muscle tissue, yellow arrowhead: fat tissue

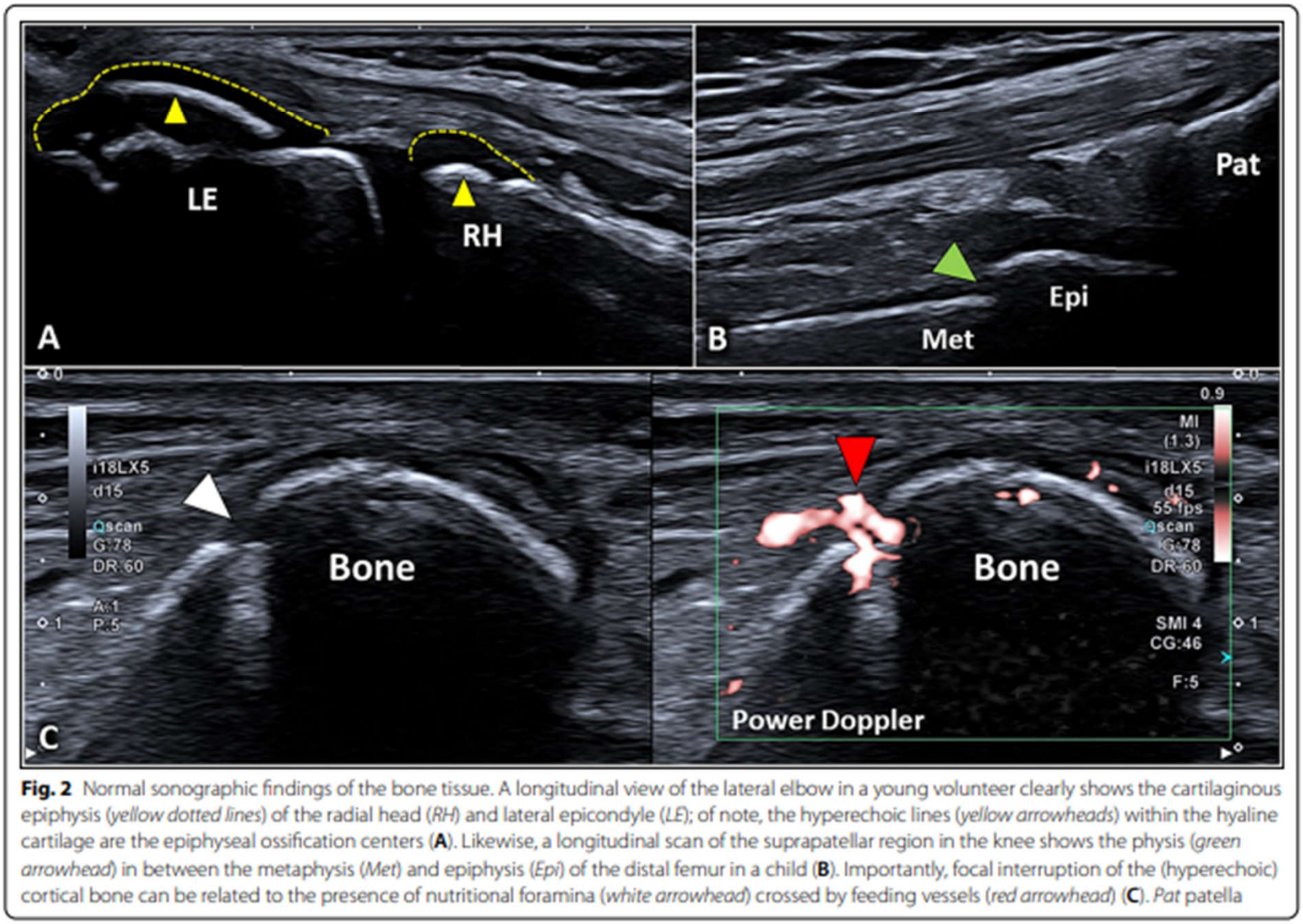

Fig. 2 Normal sonographic findings of the bone tissue. A longitudinal view of the lateral elbow in a young volunteer clearly shows the cartilaginous epiphysis (*yellow dotted lines*) of the radial head (*RH*) and lateral epicondyle (*LE*); of note, the hyperechoic lines (*yellow arrowheads*) within the hyaline cartilage are the epiphyseal ossification centers (**A**). Likewise, a longitudinal scan of the suprapatellar region in the knee shows the physis (*green arrowhead*) in between the metaphysis (*Met*) and epiphysis (*Epi*) of the distal femur in a child (**B**). Importantly, focal interruption of the (hyperechoic) cortical bone can be related to the presence of nutritional foramina (*white arrowhead*) crossed by feeding vessels (*red arrowhead*) (**C**). *Pat* patella

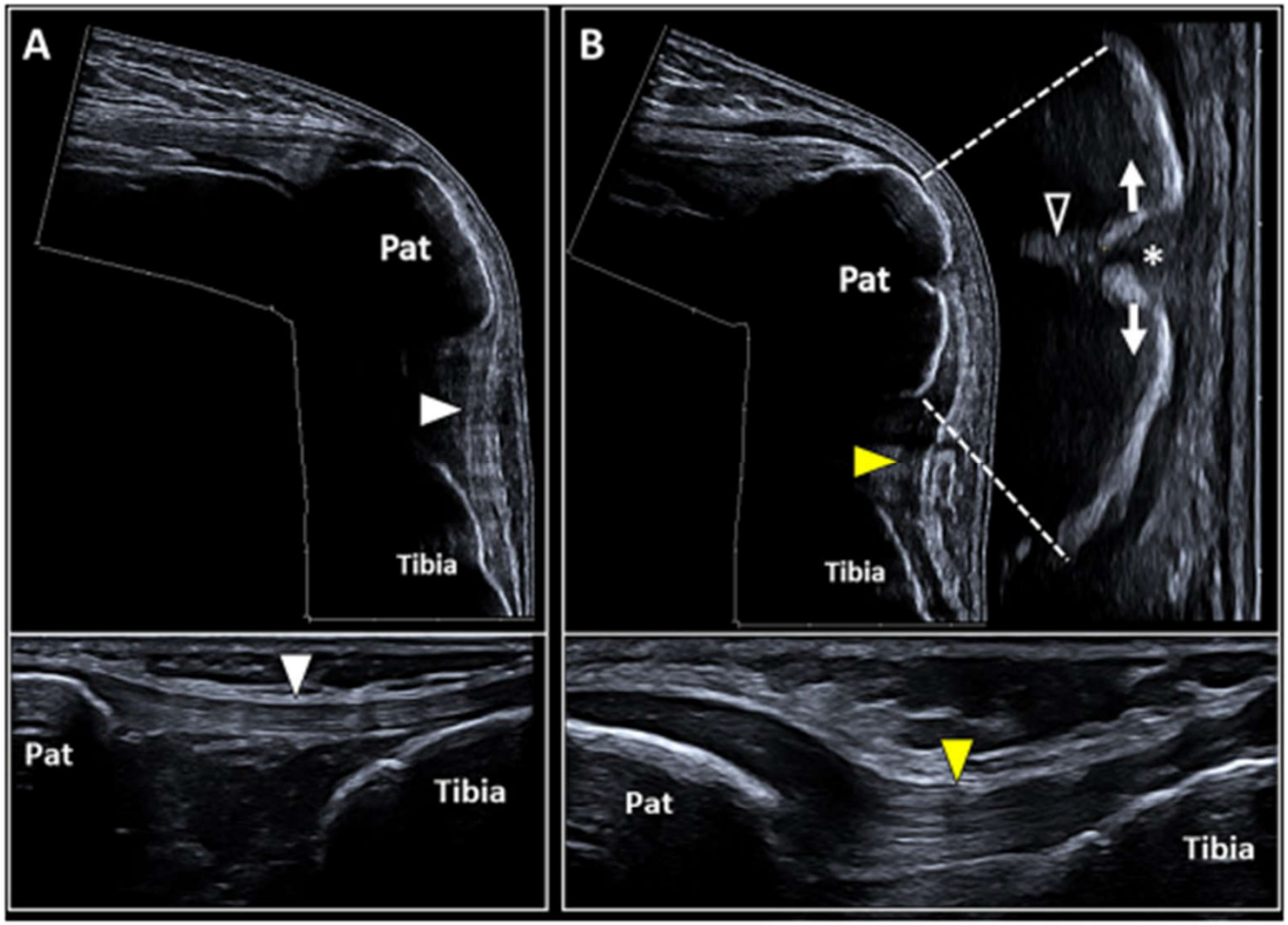

Fig. 3 Pathological sonographic findings of the bone tissue. The comparative sonographic assessment shows a continued hyperechoic cortical bone of the patella (*Pat*) with a tensioned patellar ligament (*white arrowhead*) on the healthy side (**A**); instead, cortical defect (*white asterisk*) of the patella (*Pat*), diastasis of bony fragments (*white arrows*), and deformation of the patellar ligament (*yellow arrowhead*) are clearly visible in the post-traumatic knee (**B**). Of note, the disruption of the bony cortex allows the US beam to partially penetrate within the bone tissue generating an echoic wedge (*void arrowhead*) (**B**)

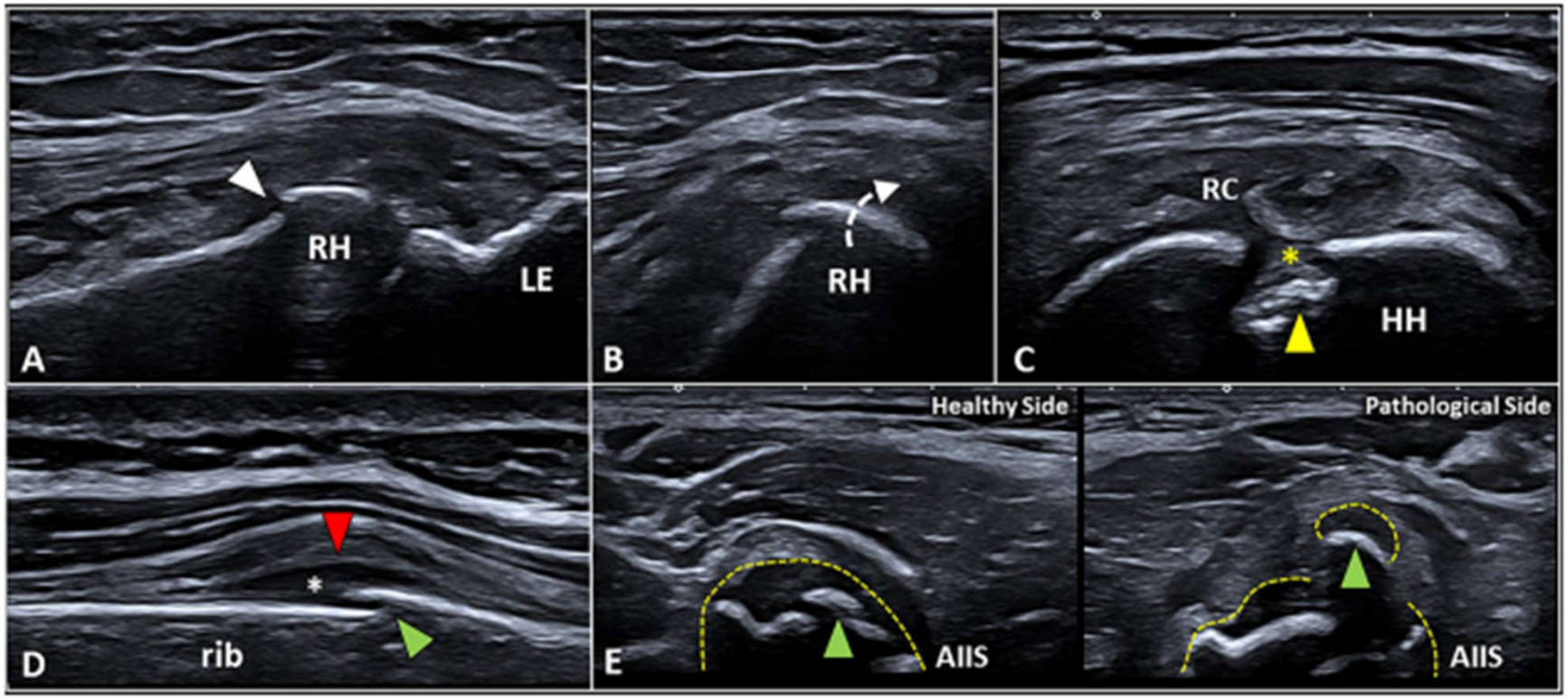

Fig. 4 Impact fractures and avulsion fractures. Longitudinal view (**A**) shows the impact fracture (*white arrowhead*) of the radial head (*RH*), but only by performing the transverse scan (**B**) the degree of rotation (*white dotted arrow*) of the bony fragment can be clearly observed. Likewise, cortical bone depression (*yellow arrowhead*) on the posterior surface of the humeral head (*HH*)—filled with fibrotic tissue (*yellow asterisk*)—can be observed in a patient with previous anterior subluxation of the shoulder (**C**). Unlike the post-acute injuries, in the acute phase of trauma (**D**) the misalignment of the cortical bone (*green arrowhead*) is usually coupled with the periosteal bulging (*red arrowhead*) and subperiosteal hematoma (*white asterisk*). Of note, avulsion fractures in the pediatric population (**E**) can show a simultaneous shifting of the cartilaginous epiphysis (*yellow dotted line*) and the epiphyseal ossification center (*green arrowhead*) located within the hyaline cartilage. *LE* lateral epicondyle, *RC* rotator cuff, *AIIS* anterior inferior iliac spine

Soft tissue abnormalities in stress fractures

ical site	Sonographic findings
um	Hypoechoic thickening of the periosteal layer
	Periosteal delamination with multi-layered pattern
	Hypo/anechoic subperiosteal effusion *
	Hypervascularization of the periosteum (color/power Doppler)
ial soft tissues	Dermal edema and/or dilatation of lymphatic collectors of sub
	Hypervascularization of the soft tissues (color/power Doppler)

ical detachment of the periosteum from the underlying cortical bone

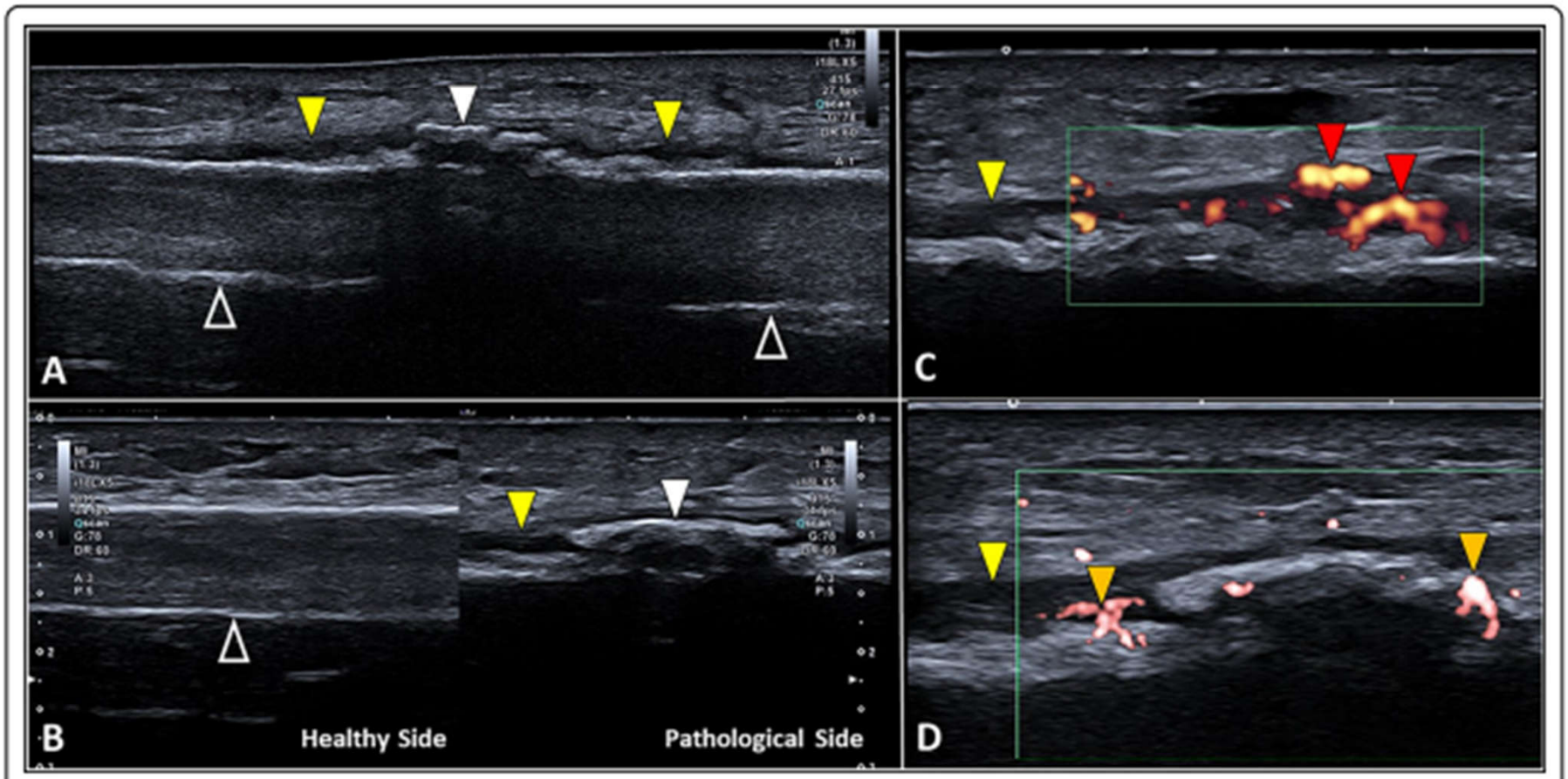

Fig. 5 Stress fractures and healing phases. Focal thickening of the periosteum (*yellow arrowhead*), the disappearance of the reverberation artifact (*void arrowheads*) of the cortical bone, and lamellar calcifications (*white arrowhead*) within the periosteum are the most common sonographic findings in the stress fractures (**A**, **B**). Using high-sensitive color Doppler to follow up the healing phases of the stress fracture, microvasculature (*red arrowheads*) within the thickened periosteum (*yellow arrowhead*) (**C**) and penetrating vessels (*orange arrowheads*) crossing through the cortical bone (**D**) can be observed

Table 2 Healing phases of bone fracture

Timing	Sonographic findings
7 days	Hypo/anechoic hematoma surrounding the fracture site
10–16 days	Hypoechoic fibrous callus within and around the fracture site
> 20 days	Hyperechoic partially-calcified callus with incomplete acoustic shadow
> 35 days	Hyperechoic calcified callus with complete acoustic shadow

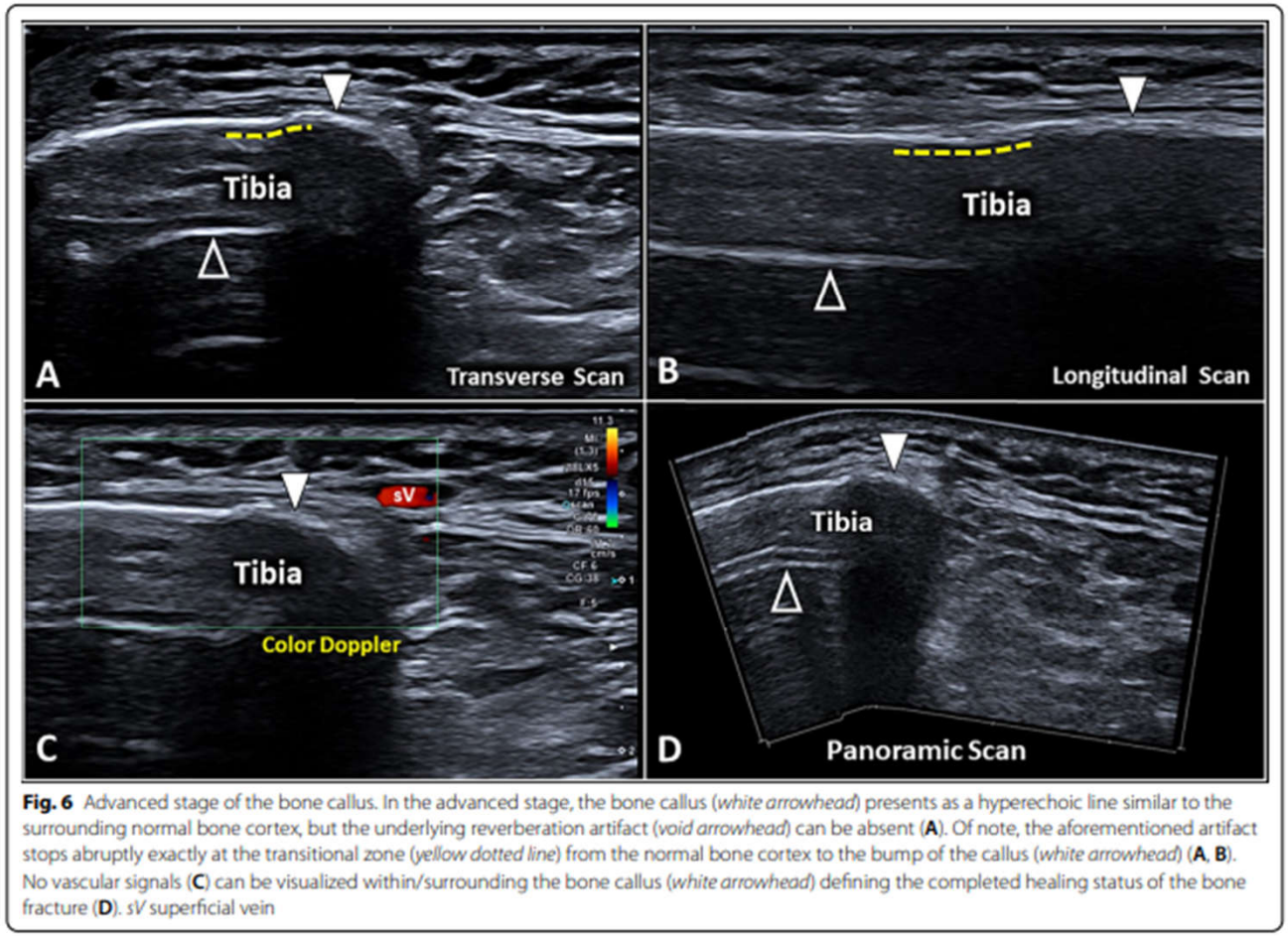

Fig. 6 Advanced stage of the bone callus. In the advanced stage, the bone callus (*white arrowhead*) presents as a hyperechoic line similar to the surrounding normal bone cortex, but the underlying reverberation artifact (*void arrowhead*) can be absent (**A**). Of note, the aforementioned artifact stops abruptly exactly at the transitional zone (*yellow dotted line*) from the normal bone cortex to the bump of the callus (*white arrowhead*) (**A**, **B**). No vascular signals (**C**) can be visualized within/surrounding the bone callus (*white arrowhead*) defining the completed healing status of the bone fracture (**D**). *sV* superficial vein

ge Journals

Search this journal | Enter search terms...

Advanced search

e by discipline | Information for

effect on point shear wave velocity elastography: Evidence in a chronic hepatitis C patient

Rizzo, Luca L'Abbate, [...], and Vincenza Calvaruso +3 View all authors and affiliations

t | https://doi.org/10.1177/1742271X231183370

nclusion:

pth is crucial for point-shear-wave elastometry performance. Excellent
gnostic performance at a depth between 4 and 5 cm can also be
tained with a smaller number of measurements than previously
commended.

tract
kground and Aims:
study investigated the depth-related bias and the influence of scan plane angle on performance of point-
ar-wave elastometry in a chronic hepatitis C patient cohort.
erials and Methods:
included 104 patients affected by chronic liver disease related to the hepatitis C virus. Liver surface nodularit
the reference to diagnose cirrhosis. The ultrasound platform was the Siemens S2000, equipped with point-
ar-wave elastometry software. Measurements were obtained in left lateral decubitus from the liver surface to
maximum depth of 8 cm in two orthogonal scan planes according to a standard sampling plane. Scatterplot
box plots explored the depth-related bias graphically. The area under the receiver operating characteristic w
d to determine the point-shear-wave elastometry diagnostic performance at progressive depths according to
surface nodularity.
ults:
he 104 patients, 68 were cirrhotics. Depth-related bias equally modified point-shear-wave elastometry in the
orthogonal scan planes. A better point-shear-wave elastometry diagnostic performance was observed
ween depths of 4 and 5 cm. The frontal scan plane assured better discrimination between cirrhotic patients a
-cirrhotic patients.
clusion:
th is crucial for point-shear-wave elastometry performance. Excellent diagnostic performance at a depth
ween 4 and 5 cm can also be obtained with a smaller number of measurements than previously recommende

MEDICAL ULTRASONOGRAPHY
An international journal of clinical imaging

An overview of ultrasound-derived radiomics and deep learning in liver

Di Zhang, Xian-Ya Zhang, Ya-Yang Duan, Christoph F Dietrich, Xin-Wu Cui, Chao-Xue Zhang

Abstract

Over the past few years, developments in artificial intelligence (AI), especially in radiomics and deep learning, have enabled the extraction of pathophysiology-related information from varied medical imaging and are progressively transforming medical practice. AI applications are extending into domains previously thought to be accessible only to human experts. Recent research has demonstrated that ultrasound-derived radiomics and deep learning represent an enticing opportunity to benefit preoperative evaluation and prognostic monitoring of diffuse and focal liver disease. This review summarizes the application of radiomics and deep learning in ultrasound liver imaging, including identifying focal liver lesions and staging of liver fibrosis, as well as the evaluation of pathobiological properties of malignant tumors and the assessment of recurrence and prognosis. Besides, we identify important hurdles that must be overcome while also discussing the challenges and opportunities of radiomics and deep learning in clinical applications.

Keywords

artificial intelligence; ultrasound; focal liver lesions; radiomics; deep learning

Ahead of print

Med Ultrason 2023:0, 1-8 Online first
DOI: 10.11152/mu-4080

An overview of ultrasound-derived radiomics and deep learning in liver

Di Zhang[1], Xian-Ya Zhang[2], Ya-Yang Duan[1], Christoph F. Dietrich[3], Xin-Wu Cui[2], Chao-Xue Zhang[1]

[1]Department of Ultrasound, The First Affiliated Hospital of Anhui Medical University, Hefei, Anhui, China, [2]Department of Medical Ultrasound, Tongji Hospital, Tongji Medical College, Huazhong University of Science and Technology, Wuhan, Hubei, China, [3]Department of Internal Medicine, Hirslanden Clinic, Bern, Switzerland

Abstract

Over the past few years, developments in artificial intelligence (AI), especially in radiomics and deep learning, have enabled the extraction of pathophysiology-related information from varied medical imaging and are progressively transforming medical practice. AI applications are extending into domains previously thought to be accessible only to human experts. Recent research has demonstrated that ultrasound-derived radiomics and deep learning represent an enticing opportunity to benefit preoperative evaluation and prognostic monitoring of diffuse and focal liver disease. This review summarizes the application of radiomics and deep learning in ultrasound liver imaging, including identifying focal liver lesions and staging of liver fibrosis, as well as the evaluation of pathobiological properties of malignant tumors and the assessment of recurrence and prognosis. Besides, we identify important hurdles that must be overcome while also discussing the challenges and opportunities of radiomics and deep learning in clinical applications.

Keywords: artificial intelligence; ultrasound; focal liver lesions; radiomics; deep learning

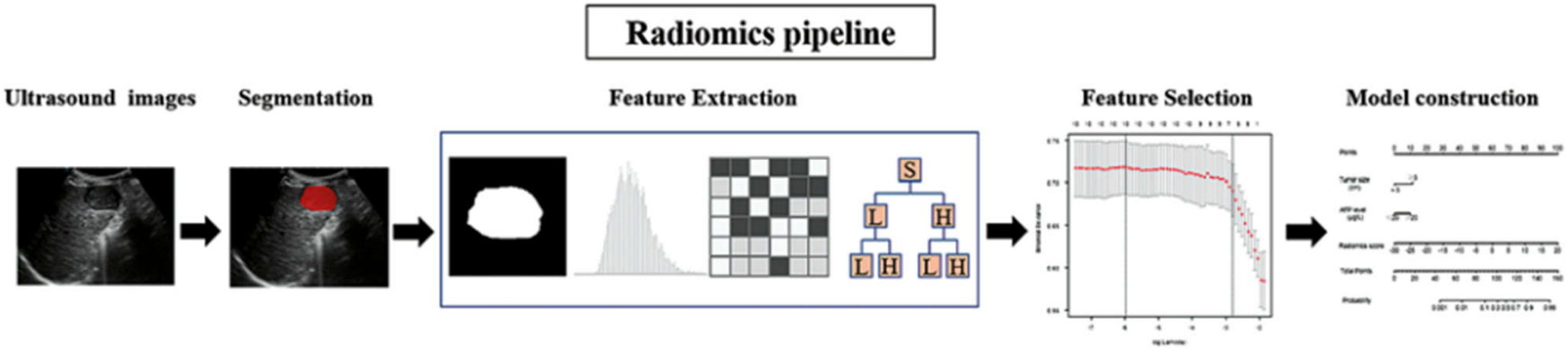

Fig 1. Schematic depiction of the radiomics workflow.

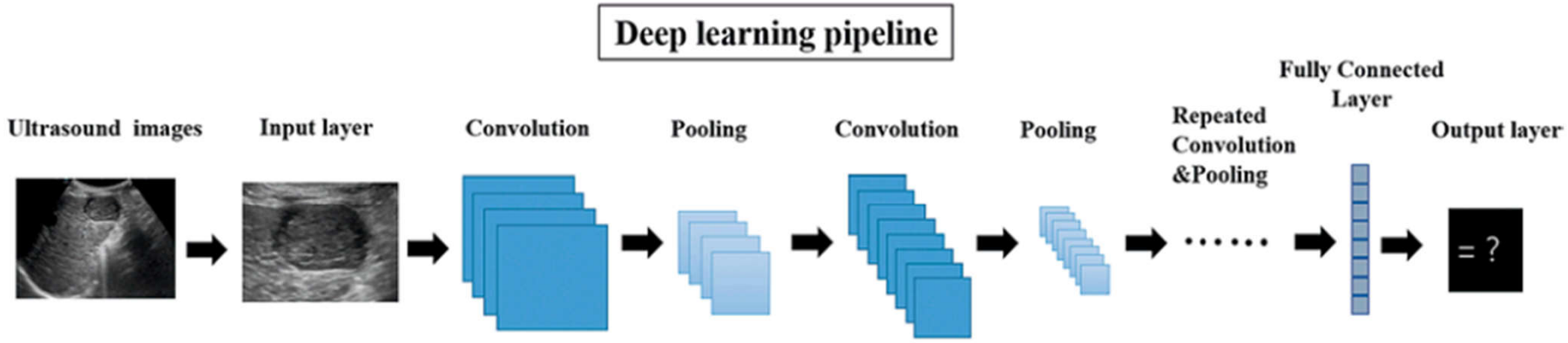

Fig 2. Framework of the simplified architecture of a convolutional neural network.

Review

Med Ultrason 2023, Vol. 25, no. 3, 330-339
DOI: 10.11152/mu-3929

Ultrasound in non-tumoral pathology of the skin

Mircea Negrutiu[1], Sorina Danescu[1], Theodor Popa[2], Adrian Baican[1]

[1]Department of Dermatology, [2]Department of Rehabilitation, "Iuliu Hatieganu" University of Medicine and Pharmacy, Cluj-Napoca, Romania

Abstract

Skin ultrasound (US) is a relatively new imaging technique, for which interest has grown significantly in the last decade. Properties such as mobility, real-time imaging and lack of irradiation or sedation, have made it a useful tool in completing the clinical examination. The use of probes of different frequencies has managed to improve the US technique, offering the possibility of obtaining high quality images. Thus, by using high-frequency and ultra-high frequency US, subclinical information can be obtained with a wide applicability in dermatological pathology. In this paper we aim to discuss the main uses of skin US in non-tumoral pathology (inflammatory and autoimmune pathology).

Keywords: ultrasound; inflammatory skin diseases; connective tissue diseases

Table I. Summary of the main ultrasound aspects in inflammatory pathologies of the skin.

Disease	Ultrasound aspect
Hidradenitis suppurativa	Bandlike anechoic or hypoechoic structures connected to the base of the hair follicle (fistulous tracts) Normal echoes (inflamed tissue) Hyperechoic linear structures (hair thread trajectories) [10]. Mixt vascular distribution (prolongued chronic evolution) [12].
Psoriasis vulgaris	Hyperechoic band that represents the epidermis Hypoechoic band that represents the elongation of the dermic papillae Hyperechoic band that is correspondent to the reticular dermis Hypoechoic band, that is correspondent to the subcutaneous tissue [17].
Lichen Planus	Hypoechoic fusiform band [29]. Thickness of the dermis higher and the density lower compared to the control tegument [30].
Septal panniculitis	Hyperechoic subcutaneous tissue, non-compressible Hypoechoic septs and increased vascular Doppler signal [33].
Cutaneous Sarcoidosis	Hypoechoic structures Heterogenous echogenicity Perilesional hyperechoic modifications Abnormal Doppler signal [35].
Keloid	Hypoechoic or heteregeneous thickness of the dermis that displaces the epidermis upwards, follows the major axis of the skin (with or without laminar pattern) and that can reach the deep tissue [38].
Autoimmune bullous diseases	PV: semi-arcuate anechoic patches in the epidermis with definite boundaries Prominent hyperechoic line at the base of the anechoic area [41]. BP: subepidermal cystic structures with dermal hypoechogenicity; Increased Doppler signal [42].
Soft tissue abscess	Well-circumscribed, hypoechoic fluid collection Peripheral hyperemia Swirling with compression Posterior acoustic enhancement Cobblestoning or branching interstitial fluid [47].

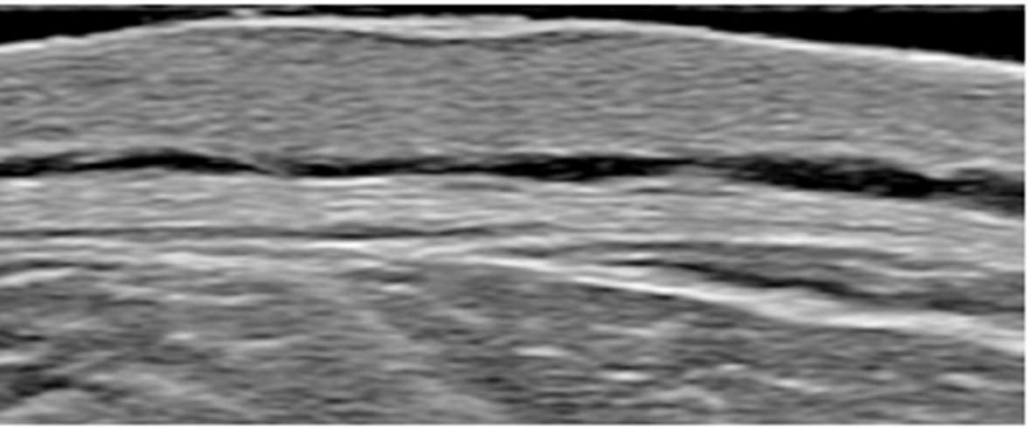

6. Discoid cutaneous lupus: HFUS shows thickening and
uced echogenicity of the dermis and increased echogenicity
l lack of fatty lobules in the subcutaneous tissue.

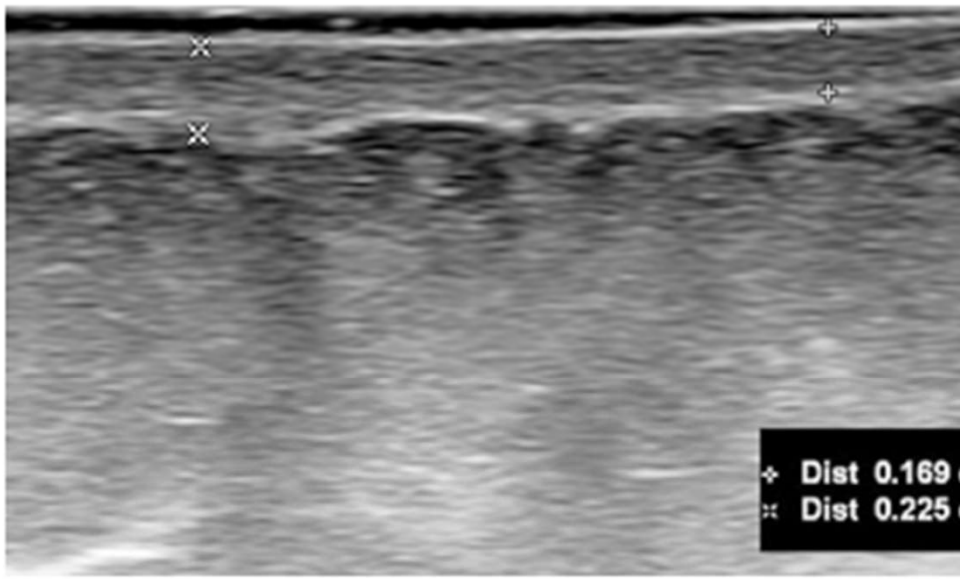

Fig 7. Atrophic morphea: HFUS shows a reduction in f
the subcutaneous tissue, a decrease in the echogenicity o
dermis and a thinning of the dermis compared to healthy s

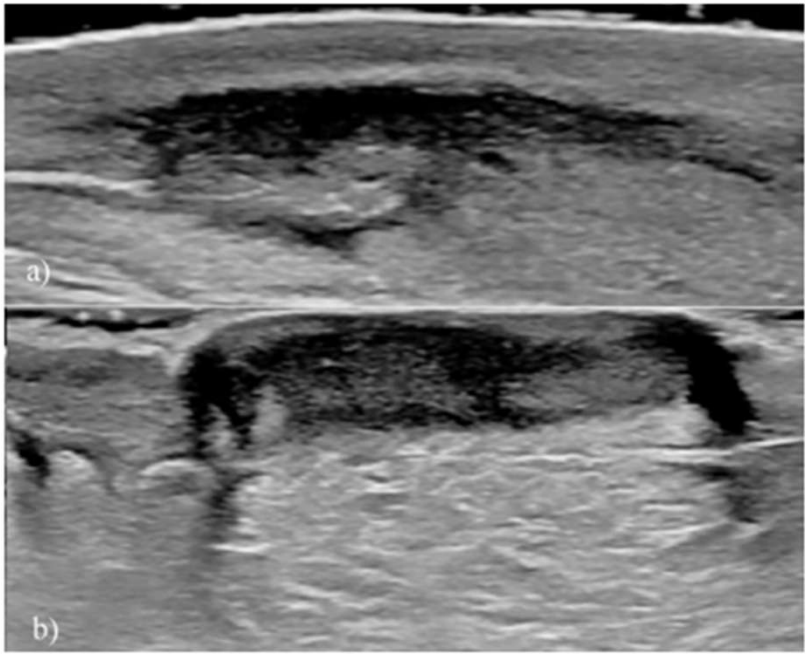

Fig 1. Hidradenitis suppurativa, HFUS shows: a) bandlike anechoic or hypoechoic structure connected to the base of the hair follicle (fistulous tract), localized in the dermis and subcutaneous tissue; b) regular and well-defined hypoechoic lesion in subcutaneous tissue, with increased echogenicity of the surrounding tissue (abscess).

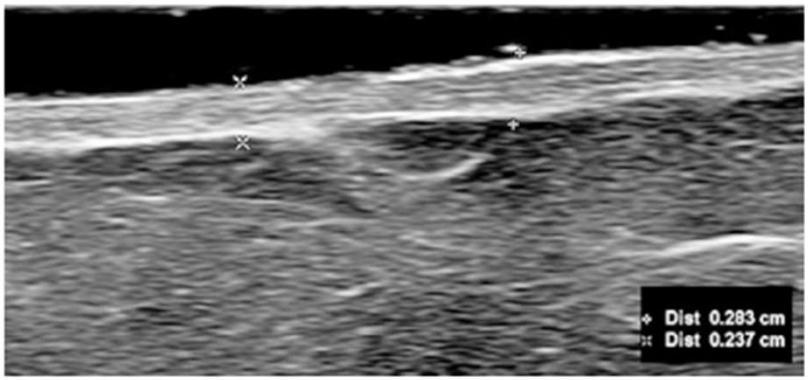

Fig 2. Psoriasis plaque: HFUS shows thickening of the epidermis and dermis compared to healthy skin, as well as hypoechoic band in the superficial dermis.

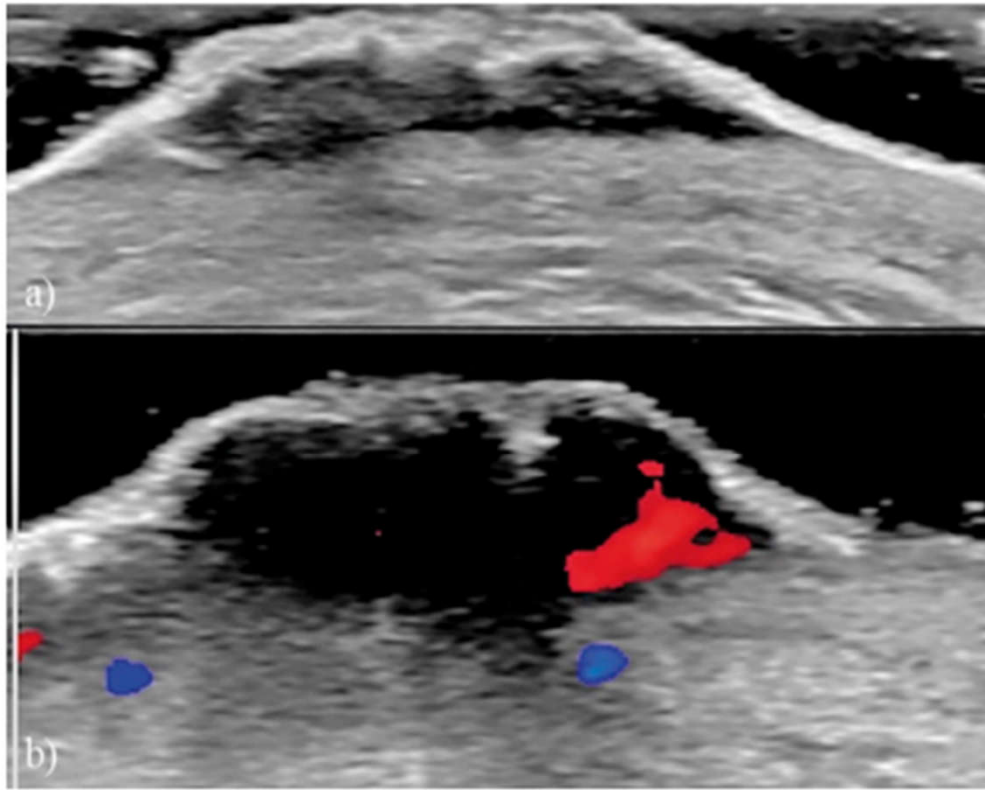

Fig 3. Hypertrophic lichen planus: a) HFUS shows a lesi involving the epidermis and dermis, with an irregular shap with poorly delimited edges, occasionally presenting anecho areas and hyperechoic spots inside. b) Color Doppler shows i creased vascularity in the lesion.

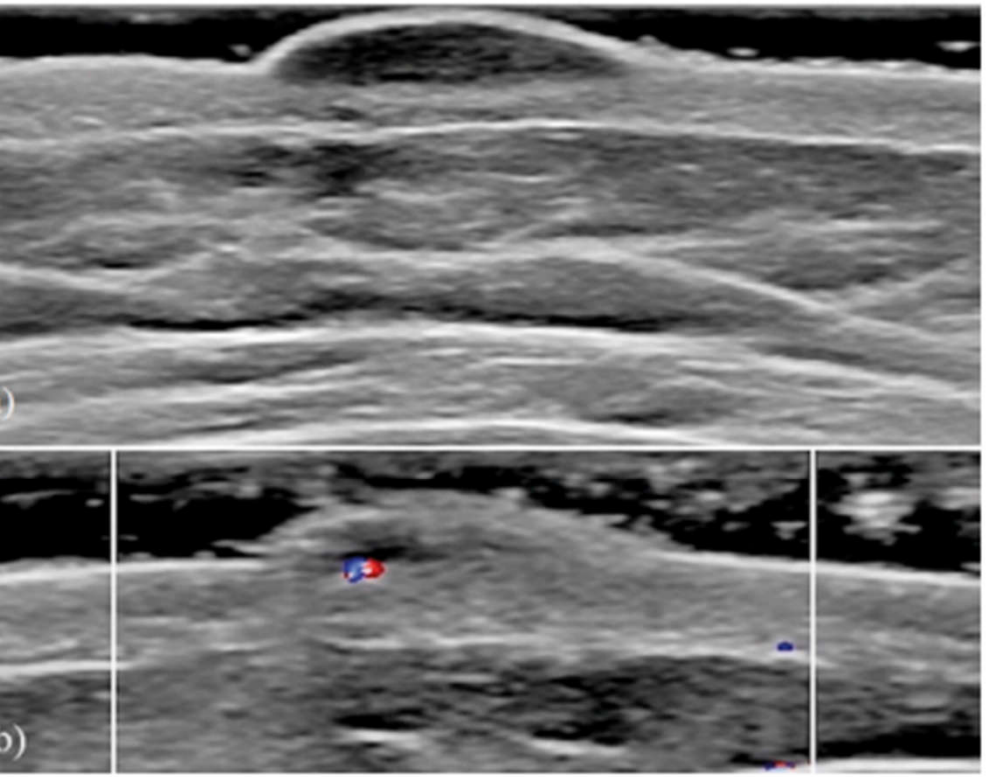

g 4. Keloid: a) HFUS shows a hypoechoic dermal structure, ell delimited, oval, with a linear fibrillar pattern; b) Color oppler shows increased vascularity in the lesion.

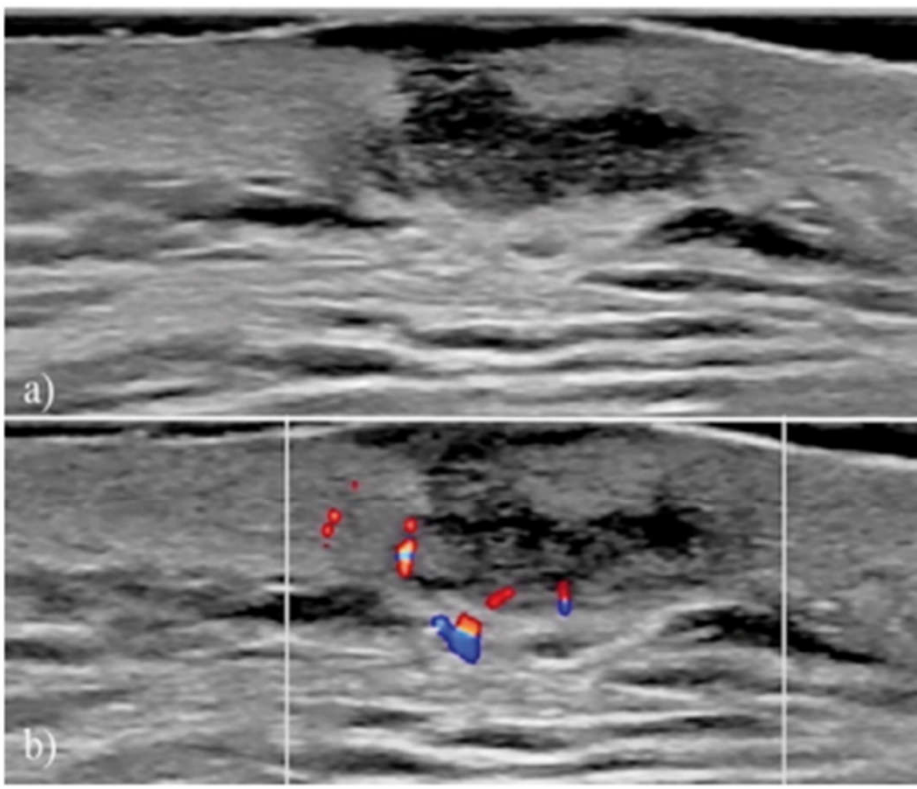

Fig 5. Abscesses: HFUS shows well-circumscribed fluid lection with heterogeneous echogenicity and posterior acc enhancement located on the upper lip. b) Color Doppler s increased vascularity in the lesion.

Table II. Summary of the main ultrasound aspects in connective tissue pathology

Disease	Ultrasound aspect
Lupus erythematosus	Inflammatory phase: Thickening of the dermis Decrease in echogenicity of the dermis Increase in the echogenicity of the subcutaneous tissue Increased Doppler signal [52].
	Atrophic phase: Decreased dermal and subcutaneous tissue thickness Decreased Doppler signal [52].
Systemic sclerosis	Oedematous phase: Dermal thickening and a reduction in echogenicity of the skin Mildly elevated skin elasticity Increased Doppler signal [41].
	Sclerotic phase: Mildly reduced thickness of the subcutaneous fat layer Increased echogenicity of the skin and subcutaneous tissue Moderately increased skin elasticity [41].
	Atrophic phase: Thinning of the dermis and subcutaneous fat layer [41].
Morphea	Inflammatory phase: Loss of definition of dermic-hypodermic junction Expression of the hypodermic diffuse or partial echogenicity Hypervascularization of dermis and hypodermis [67].
	Inactive phase: Thinning of dermis and hypodermis with areas that lost adipose subcutaneous tissue The dermis coming in direct contact with the fascia [67].
	Final stage: Dermis and hypodermis show high echogenicity with a fibrillary pattern [67].